



Structural and electrical properties of rare earth (R^{3+}) doped Cobalt ferrites

P. K. Gaikwad^a, S. S. Sawant^b

^aDepartment of Physics, B.S.S. Art's, Science and Commerce College, Makni (M.S.)- 413604 India.

^bDepartment of Physics, Shri Chhatrapati Shivaji College, Omerga (M.S.)- 413606 India.

Abstract: Rare earth (R^{3+}) doped cobalt ferrite materials with chemical formula $CoFe_{2-x}R_xO_4$ ($x = 0.00$ and 0.02 where $R^{3+} = Sm^{3+}, Nd^{3+}, Dy^{3+}$) have been synthesized by standard ceramic technique using AR grade CoO , Dy_2O_3 , Sm_2O_3 , Nd_2O_3 , and Fe_2O_3 . The X-ray diffraction (XRD) measurements confirmed the formation of a single-phase cubic spinel structure. The unit cell volume, particle size, hopping length and lattice constant decreases, while the X-ray density, bulk density, porosity increases with rare earth doped cobalt ferrite. Electrical conductivity was investigated from two probe technique in the temperature range 300K to 850K. Plots of $\log\rho(\Omega m)$ vs $1000/T K^{-1}$ reciprocal of temperature shows a transition near the Curie temperature. Activation energy and D.C. electrical resistivity both are decreases with doped rare earth (R^{3+}) ions in cobalt ferrites and activation energy in the paramagnetic region is more than that of ferrimagnetic region.

Keywords: Cobalt ferrite, rare earths, Structural and Electrical properties.

1. Introduction:

Spinel ferrites with the general formula MFe_2O_4 (M is divalent metal cation) are attracted much attention in recent years because of their potential applications in high density magnetic recording, magnetic fluids, spintronics, data storage, and gas sensors [1–3]. Among the ferrite nanoparticles, cobalt ferrite has been widely studied due to its excellent chemical stability, mechanical hardness, reasonable saturation magnetization, and high magneto-crystalline anisotropy. These properties make it a promising candidate for many applications, namely, magnetic data storage, magnetic drug targeting, biosensors, and magnetic refrigeration, digital diaries, video camera, recorder, floppy drives, computer electromagnetic interference (EMI) remote control, inductors, electronics watches, TV/ computer games and audio system etc. Which have high resistivity and low eddy current losses are used as microwave devices such as isolators and phase shifters inductor memory core high frequency transformers and recording heads [4–7]. The important electrical and magnetic properties of ferrite depend on chemical compositions, method of preparation and cation distribution in the two sub-lattices i.e. tetrahedral (A)

and octahedral [B] site. The study of cation distribution in spinel ferrites is essential to understand structural and magnetic properties of spinel ferrites [8, 9].

In the family of spinel ferrites CoFe_2O_4 is a unique ferrite having inverse spinel structure. CoFe_2O_4 is a hard magnetic material possessing high magneto crystalline anisotropy, high Curie temperature, high corecivity and moderate saturation magnetization along with the chemical stability and mechanical hardness [10, 11]. Several researchers have studied pure and substituted cobalt ferrite with a view to understand their basic properties [12-14].

Spinel with rare earth ions has attracted great alternations in the material science field because of their interesting properties such as infrared emission, catalytic, photoelectric and magnetic properties [15, 16]. Many investigations have been carried out to make further improvements on the structural and magnetic properties of substituted ferrites. It is known that the rare earth (RE) ions have unpaired 4f electrons which have the role of originating magnetic anisotropy because of their orbital shape. Doping of rare earth ions into spinel ferrites, the occurrence of 4f-3d coupling which determine the magneto crystalline anisotropy in ferrites can also improve the electrical and magnetic properties of spinel ferrites.

Recent research shows by introducing rare earth ions into the spinel lattice, can lead to small changes in the structural, magnetization and Curie temperature of the spinel ferrite [17-18]. In the present work, we report our result on the structural and electrical properties of rare earth (R^{3+}) doped cobalt ferrites.

2. Experimental details:

Samples with chemical formula $\text{CoFe}_{2-x}\text{R}_x\text{O}_4$ ($x = 0.00$ and 0.02 where $\text{R}^{3+} = \text{Dy}^{3+}, \text{Sm}^{3+}, \text{Nd}^{3+}$) were prepared by standard ceramic technique [20] using analytical reagent grade oxides. Compounds were accurately weighted in molecular weight percentage with single pan microbalance. The mixed powders were wet ground and pre-sintered at 950°C for 24 hours. The sintered powder is again re-ground and pelletized. Polyvinyl alcohol was used as a binder in making circular pellets of 10mm diameter and 2–3mm thickness. The pellets were finally sintered in muffle furnace for 1180°C for 24 hours and then slowly cooled to the room temperature.

X-Ray diffraction patterns were taken at room temperature to confirm the crystal structure of the prepared samples. The XRD patterns were recorded in the 2θ range from 20° to 80° using $\text{Cu-K}\alpha$ radiation ($\lambda = 1.5406 \text{ \AA}$) with scanning rate 2° per/m.

The temperature dependence of D.C. electrical resistivities of disc shaped pellets are using two probe-technique in the temperature range 300K to 850K with step of 10K and for good electrical ohmic contact the pellets were polished and silver pasted on both the surface.

3. Results and Discussion:

3.1 Structural analysis: Room temperature X-ray powder diffraction patterns (XRD) for series having molecular formula $\text{CoFe}_{2-x}\text{R}_x\text{O}_4$ were ($x=0.00$ and $x=0.02$ where $\text{R}^{3+} = \text{Dy}^{3+}, \text{Sm}^{3+}, \text{Nd}^{3+}$) prepared by standard ceramic technique shown in Fig 1.

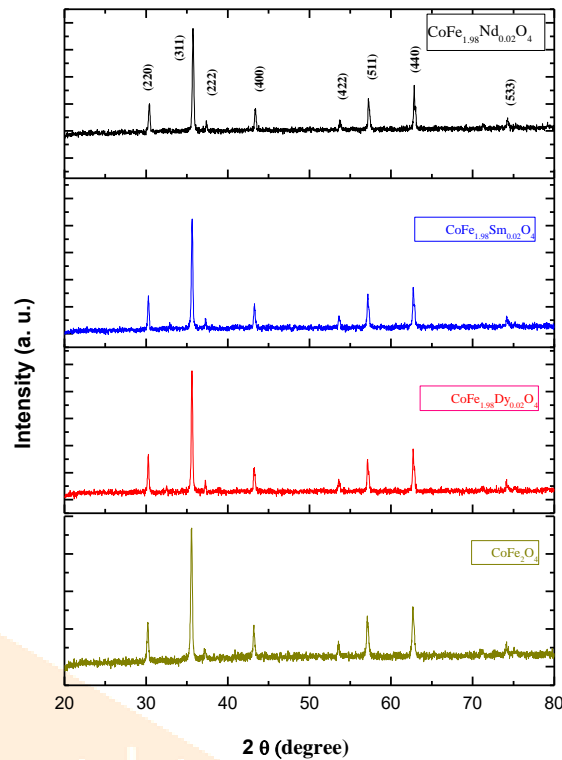


Fig 1: XRD patterns of $\text{CoFe}_{2-x}\text{R}_x\text{O}_4$ ($x = 0.00$ & 0.02 where $\text{R}^{3+} = \text{Dy}^{3+}, \text{Sm}^{3+}, \text{Nd}^{3+}$)

The Braggs reflections (hkl) belonging to the plane (220), (311), (222), (400), (422), (511), (440) and (533) confirms the formation of single-phase cubic spinel structures. No extra peak of rare earth doped CoFe_2O_4 materials is observed for $x = 0.02$. Similar reports of XRD pattern are available in the literature [21-23].

Table 1: Lattice constant (a), X- ray density (d_x), bulk density (d_B), Porosity (P) and Particle size (t) of $\text{CoFe}_{2-x}\text{R}_x\text{O}_4$ system.

$\text{CoFe}_{2-x}\text{R}_x\text{O}_4$	'a'	'a ³ '	Dx	d _B	P	T
	(Å)	(Å) ³	(gm/cm ³)	(gm/cm ³)	(%)	(Å)
CoFe_2O_4	8.376	587.64	5.305	3.864	27.16	396.71
$\text{CoFe}_{1.98}\text{Dy}_{0.02}\text{O}_4$	8.369	586.16	5.305	3.864	27.16	417.40
$\text{CoFe}_{1.98}\text{Sm}_{0.02}\text{O}_4$	8.362	584.70	5.373	3.866	28.05	395.47
$\text{CoFe}_{1.98}\text{Nd}_{0.02}\text{O}_4$	8.343	580.72	5.407	3.877	28.30	395.59

Using XRD data the lattice constant (a) was calculated using standard relation for cubic spinel structure. The values of lattice constant are given in Table 1 that the lattice constant of rare earth doped CoFe_2O_4 is less than pure CoFe_2O_4 . A minor-decreases in lattice parameter, α_0 of CoFe_2O_4 with rare earth doped, which may be due to the compressive pressure exerted on the ferrite lattice by $\text{R}^{3+}\text{FeO}_3$ [24]. The X-ray density (d_x) was calculated using the equation

$$d_x = \frac{ZM}{N a^3} \quad \dots(1)$$

Where 'Z' is number of molecules per unit cell. (For spinel system Z= 8), 'M' is the molar mass of the ferrite, 'N_a' is the Avogadro's number and 'a³' is the unit cell volume computed from the values of lattice constant. X-ray density (d_x) increases almost linearly with the doped of R³⁺ because the Fe³⁺ ions on the octahedral sites are being replaced by the larger mass R³⁺ ions.

The bulk density of the samples was measured by using Archimedes principle [25] and values are presented in Table 1. The porosity of the samples was calculated by using the following relation and values are tabulated in Table 1.

$$p = \left(1 - \frac{d_B}{d_x} \right) \times 100\% \quad \dots(2)$$

where d_B is the bulk density and d_x is X-ray density.

The particle size 't' of sample was determined by most intense peak (311) by using the relation

$$t = \frac{0.9\lambda}{\beta \cos \theta} \quad \dots(3)$$

Where β the full width at half maximum (FWHM) and λ is is wavelength of the target material. The particle size values are given in Table 1. It is observed from table 1 that the particle size of rare earth doped is smaller than the pure CoFe₂O₄.

The values of the tetrahedral and octahedral bondlength (d_{AX} and d_{BX}), the tetrahedral edge (d_{AXE}), and the shared and unshared octahedral edge (d_{BEX} and d_{BXEU}) can be calculated according Eqs (4) ~ (8). Using the value of the lattice parameter 'a' (Å) and the oxygen position parameter 'u' (u=0.381 Å). The value of the bondlength of the tetrahedral and octahedral sites are shown in Table 2, It is seen that the all values are depend on the lattice parameter so, the lattice parameter decrease, then the edge and the bondlength of the tetrahedral and octahedral sites are decreases.

$$d_{AX} = a\sqrt{3}\left(u - \frac{1}{4}\right) \quad \dots(4)$$

$$d_{BX} = a\left[3u^2 - \left(\frac{11}{4}\right)u + \left(\frac{43}{64}\right)\right]^{\frac{1}{2}} \quad \dots(5)$$

$$d_{AXE} = a\sqrt{2}\left(2u - \frac{1}{2}\right) \quad \dots(6)$$

$$d_{BAX} = a\sqrt{2}(1 - 2u) \quad \dots(7)$$

$$d_{BXEU} = a\left[4u^2 - 3u + \left(\frac{11}{16}\right)\right]^{\frac{1}{2}} \quad \dots(8)$$

The distance between magnetic ions (hopping length) in the tetrahedral sites is given by Eqs (9) ~ (10).

$$L_A = \frac{a\sqrt{3}}{4} \quad \dots(9)$$

$$L_B = \frac{a\sqrt{2}}{4} \quad \dots(10)$$

where 'a' is the lattice constant, the value Hopping length (L_A , L_B) are shown in Table 2, Hopping length (L_A , L_B) values are depend on the lattice parameter so that the lattice parameter are decrease so the Hopping length (L_A , L_B) also decreases.

Table 2: Hopping length (L_A , L_B), Tetrahedral bond (d_{AX}), Octahedral bond (d_{BX}), tetra edge (d_{AXE}) and octaedge (d_{BXE}) (Shared and non-shared) of $\text{CoFe}_{2-x}\text{R}_x\text{O}_4$ system.

$\text{CoFe}_{2-x}\text{R}_x\text{O}_4$	L_A (Å)	L_B (Å)	d_{AX} (Å)	d_{BX} (Å)	d_{AXE} (Å)	d_{AXE} (Å)	
						(Shared)	(Unshared)
CoFe_2O_4	3.629	2.961	1.901	2.045	3.103	2.819	2.963
$\text{CoFe}_{1.98}\text{Dy}_{0.02}\text{O}_4$	3.629	2.959	1.899	2.043	3.101	2.817	2.961
$\text{CoFe}_{1.98}\text{Sm}_{0.02}\text{O}_4$	3.621	2.956	1.897	2.042	3.098	2.815	2.958
$\text{CoFe}_{1.98}\text{Nd}_{0.02}\text{O}_4$	3.613	2.950	1.893	2.037	3.091	2.808	2.952

3.2. D.C. resistivity

The D.C. electrical resistivity (ρ) of both the sample was calculated by measuring the resistivity 'R' of the samples. The variations of logarithm of resistivity ($\log \rho$) with temperature for both the samples. A change in slope is observed in the resistivity curve dividing the curve in two regions corresponding to ferrimagnetic region and paramagnetic region for both the samples as shown in Fig 2.

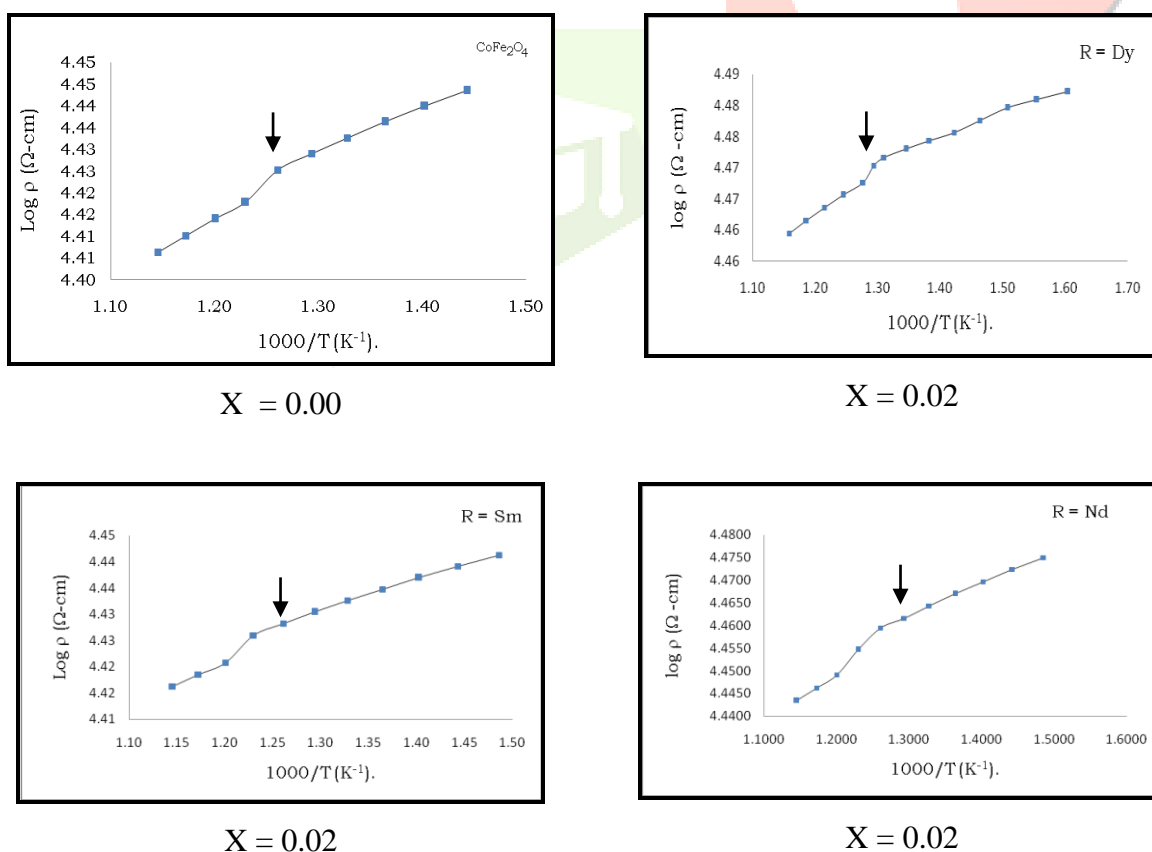


Fig 2: Variation of $\log \rho$ Vs $1000/T$ (K⁻¹) of $\text{CoFe}_{2-x}\text{R}_x\text{O}_4$

The temperature at which slope of the curve change. Corresponds to the Curie temperature of the sample. The resistivity plots obeys the exponential relation by

$$\rho = \rho_0 \exp\left(\frac{\Delta E}{kT}\right) \quad \dots(11)$$

Where, ρ_0 is the temperature dependent factor, ΔE is the activation energy and k is the Boltzmann constant. Taking the slope of the resistivity graphs and using above equation activation energy of both the samples corresponding to paramagnetic region and ferrimagnetic region was calculated. The value of paramagnetic region is graters than that of ferromagnetic region as shown in Table 3 [26, 27]. D.C. resistivity and activation energy will be change with doped R^{3+} rare earth ion in cobalt ferrite. Table. 3 shows that the variation of D. C. resistivity and activation energy both are decreases with rare earth (R^{3+}) doped content in cobalt ferrite.

Table 3: Activation energy in paramagnetic (E_p), Ferrimagnetic (E_f) and Activation energy (ΔE) region of $CoFe_{1.98}R_{0.02}O_4$ system.

$CoFe_{2-x}R_xO_4$	E_p	E_f (\AA) ³	ΔE (gm/cm^3)	D. C. Resistivity
$CoFe_2O_4$	0.690	0.320	0.370	793
$CoFe_{1.98}Dy_{0.02}O_4$	0.596	0.286	0.310	773
$CoFe_{1.98}Sm_{0.02}O_4$	0.611	0.298	0.313	783
$CoFe_{1.98}Nd_{0.02}O_4$	0.616	0.301	0.315	763

The decrease in resistivity may be attributed to the fact that the ionic radius of Dy^{3+} (0.908 \AA), Sm^{3+} (0.964 \AA), Nd^{3+} (0.995 \AA) is larger than that of Fe^{3+} (0.67 \AA) and when the (R^{3+}) rare earth doped for Fe^{3+} , a part of (R^{3+}) rare earth will occupy octahedral sites leading to replacement of Fe^{3+} ions from octahedral sites.

4. Conclusions:

In present investigation indicate that the $CoFe_{2-x}R_xO_4$ ($x = 0.00$ and 0.02 where $R^{3+} = Dy^{3+}, Sm^{3+}, Nd^{3+}$) spinel ferrite system was successfully prepared by standard ceramic technique. The X-ray powder diffraction analysis of the samples revealed that the prepared sample possesses single phase cubic spinel structure. The lattice constant, particle size decreases but X-ray density, bulk density and porosity increases with rare earth doped Cobalt ferrites. Hopping length, tetrahedral bond, Octahedral bond, tetra edge and octa edge are decreases with rare earth doped Cobalt ferrites. Activation energy and D. C. electrical resistivity both are decreases with doped (R^{3+}) rare earth ions in cobalt ferrites and activation energy in paramagnetic region is more than that of ferrimagnetic region.

References:

- [1] M. Ishaqu, M. U. Islam, M. A. Khan I. Z. Rahman A. Genson, S. Hampshire
Physica B 405(2010) 1532.
- [2] B. P. Jacob, S. Thankachan, S. Xavier, and E. M. Mohammed, “Dielectric behaviour and AC conductivity of Tb³⁺ doped Ni_{0.4}Zn_{0.6}Fe₂O₄ nanoparticles,” Journal of Alloys and Compounds, vol. 541, pp. 29–35, 2012.
- [3] S. Thankachan, B. P. Jacob, S. Xavier, and E. M. Mohammed, “Effect of neodymium substitution on structural and magnetic properties of magnesium ferrite nanoparticles,” Physica Scripta, vol. 87, no. 2, Article ID 025701, 2013.
- [4] L. B. Tahar, M. Artus, S. Ammar et al., “Magnetic properties of CoFe_{1.9}RE_{0.1}O₄ nanoparticles (RE = La, Ce, Nd, Sm, Eu, Gd, Tb, Ho) prepared in polyol,” Journal of Magnetism and Magnetic Materials, vol. 320, no. 23, pp. 3242–3250, 2008.
- [5] E. V. Gopalan, P. A. Joy, I. A. Al-Omari, D. S. Kumar, Y. Yoshida, and M. R. Anantharaman, “On the structural, magnetic and electrical properties of sol-gel derived nanosized cobalt ferrite,” Journal of Alloys and Compounds, vol. 485, no. 1-2, pp. 711–717, 2009.
- [6] B. G. Toksha, S. E. Shirsath, S. M. Patange, and K. M. Jadhav, “Structural investigations and magnetic properties of cobalt ferrite nanoparticles prepared by sol-gel auto combustion method,” Solid State Communications, vol. 147, no. 11-12, pp. 479–483, 2008.
- [7] Z. Zi, Y. Sun, X. Zhu, Z. Yang, J. Dai, and W. Song, “Synthesis and magnetic properties of CoFe₂O₄ ferrite nanoparticles,” Journal of Magnetism and Magnetic Materials, vol. 321, no. 9, pp. 1251–1255, 2009.
- [8] E. V. Gopalan, I. A. Al-Omari, D. S. Kumar, Y. Yoshida, P. A. Joy, and M. R. Anantharaman, “Inverse magnetocaloric effect in sol-gel derived nanosized cobalt ferrite,” Applied Physics A, vol. 99, no. 2, pp. 497–503, 2010.
- [9] L. Gama, A.P. Diniz, A.C.F.M. Costa, S.M. Rezende, A. Azevedo, D.R. Cornejo Physica B 384 (2006) 97.
- [10] J. Peng, M. Hojamberdiev, Y. Xu, B. Cao, J. Wang, H. Wu.
J. Magn. Mater. 323(2011) 133.
- [11] P. S. Aghav, V. N. Dhage, M. L. Mane, D. R. Shengule, R. G. Dorik, K. M. Jadhav.
Physica B 406(2011) 4350.
- [12] I. P. Muthuselvam, R.N. Bhowmik J. Magn. Mater. 322 (2010) 767.
- [13] C. Yan, F. Cheng, Z. Peng, Z. Xu, and C. Liao
J. Appl. Phys. 84 (1998) 10.
- [14] M Maisnam, S Phanjobam, H.N.K. Sarma, C Prakash, L. R Devi, O.P. Thakur Physica B 370 (2005) 1.

- [15] Y. M. Al Angari J. Magn. Mater. 323 (2011) 1835.
- [16] M. A. Ahmed, E. Ateia, F. M. Salem. Physica B 381 (2006) 144.
- [17] K. K. Bharathi, R. S. Vemuri, C. V. Ramana. Chem. Phys. Lett. 504 (2011) 202.
- [18] K. K. Bharathi, J. A. Chelvane, G. Markandeyulu. J. Magn. Mater. 321 (2009) 3677.
- [19] E. E. Sileo, S. E. Jacobo. Physica B 354 (2004) 241.
- [20] D. R. Patil, B. K. Chougule. Mater. Chem. Phys. 117 (2009) 35.
- [21] Mansor Al-Haj. J. Magn. Mater 299(2006) 435.
- [22] S. Jie, W. Lixi, X. Naicen, Z. Qitu. J. Rare Earths 28(2010) 451.
- [23] J. Jiang, Y. Yang, L. Li. Physica B. 399 (2007) 105.
- [24] P. K. Roy, J. Bera. J. Magn. Mater 321 (2009) 247.
- [25] M. L. Mane, R. Sundar, K. Ranganathan, S. M. Oak, K. M. Jadhav. Nucl. Instrum. Methods B 269 (2011) 466.
- [26] K. V. Kumar and D. Ravinder, Mater. Lett. 52 (2002) 166.
- [27] D. Ravinder. and B. R. Kumar, Mater. Lett. 57 (2003) 1738.

